Lab #5 – Detecting Exoplanet Transits

AST326 – March 20, 2019

Ayush Pandhi (ayush.pandhi@mail.utoronto.ca)

Group C: Ayush Pandhi and Hansen Jiang

1 Abstract

The detection and study of exoplanets is a large branch of astronomy and in this experiment, optical data from the William Herschel Telescope (WHT) for a field of view containing GJ1214 are analyzed. Systemic corrections are applied corresponding to the bias and flat field sets from the Auxiliary-port Camera (ACAM) and a light curve is generated by comparing the flux of the target star (GJ1214a) over time with respect to the flux of six selected reference stars in the field whose flux is known to not vary drastically over time (i.e. they are not known variable stars). The light curve of the transit system is them analyzed to obtain estimates of the radius, density, period, orbital distance, impact parameter and inclination angle of the exoplanet GJ1214b; the conditions of the system and classification of the planet is discussed. Overall, the goal of this experiment was to better understand the detection of exoplanets using the transit method through a study on a well-known system.

2 Introduction

The universe has a plethora of stars, with approximately 250 billion just in the Milky Way. While astronomers study in detail these bright objects, learning all of their properties and how they move through the sky, there are other objects that are not as visible that still pique their interest. Similar to our own solar system, a lot of stars that are observed also have planets orbiting them and the detection and study of these planets is an entire branch of astronomy itself. While exoplanets themselves are not bright enough to be observed directly, there are a multitude of methods through which astronomers can find them, some of them include:

i) Radial Velocity – Parent stars are affected by the gravitational effects of their planets and thus have their own small orbit which can be detected through a Doppler shift in the star's spectral emission.

ii) Direct Imaging – For especially large exoplanets relatively nearby and on large orbits around their parent star, it is possible to directly observe them in the infrared, although this is not widely applicable in most scenarios.

iii) Gravitational Microlensing – A spike of luminosity observed when a planet gravitationally lenses its parent star; this technique is particularly useful when looking at exoplanets at large distances.

iv) Pulsar Timing – Slight variations in a pulsar's rotation can be used to measure the object's orbital motion due to a companion exoplanet. Although, it is a rare case to have a pulsar-planetary system and such a system is most likely not habitable.

v) Transit – The most common detection method; when a planet eclipses its parent star, the observed luminosity from the star decreases and as such a light curve with a clear dip can be seen for systems with exoplanets.

Although there are other methods to detect exoplanets, these are the most commonly used (Figure 1).

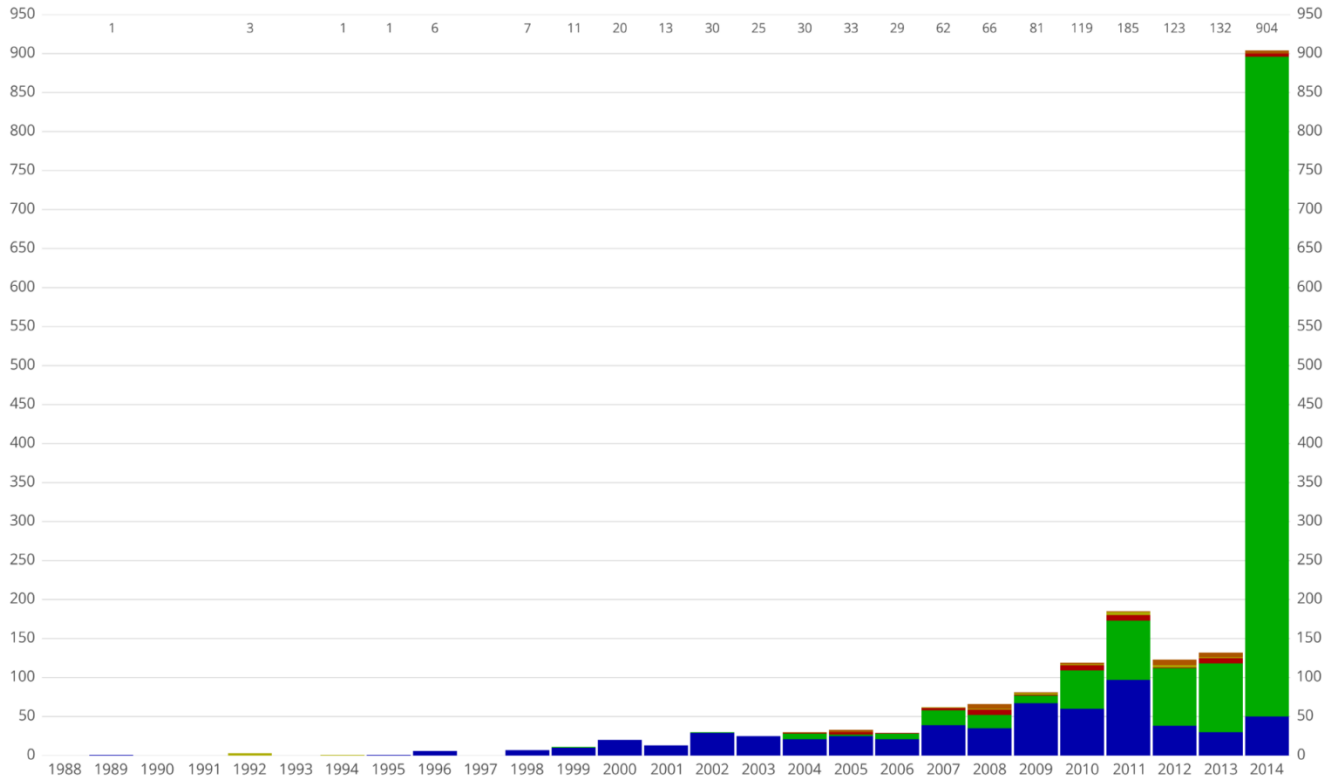

Figure 1: *Total number of exoplanets detected every year since 1988, colour coded by which method was used to detect them (green = transit, blue = radial velocity, red = direct imaging, brown = microlensing, yellow = pulsar timing). The large number of exoplanets found in 2014 corresponds primarily to the Kepler Space Telescope's findings.*

The following experiment uses data gathered from the William Herschel Telescope (WHT) for the GJ1214 system as well as other nearby stars in the sky[8]. Through a data correction process using provided bias and flat field data, the flux of GJ1214a is plotted with respect to selected reference stars. This generates a light curve that allows for the study of multiple properties of the system (transit depth, the planet's radius and density, etc.) using the transit photometry method. The light curve is also

studied with the consideration of limb darkening – an optical effect such that the edges of stars is dimmer than the center.

3 Observation and Data

The data sets used for this experiment were taken by the Isaac Newton Group using the Auxiliary-port Camera (ACAM) on the William Herschel Telescope. The telescope is located in the Canary Islands in Spain (La Palma island) at (28°45′38″ N, 17°52′54″ W) in terms of latitude and longitude and is at an altitude of 2344 m. The ACAM is an optical instrument with broad and narrow band imaging capabilities with a field of view of approximately 8 arcminutes across; the resolution for this instrument is roughly 0.25 arcsec/pixel. The set of data that will be used for this experiment specifically was taken on August 23, 2011 between 14:46 and 6:01 (UT) with a total collection time of 15.25 hours. The specific observation conditions as well as comments are recorded and provided by the Isaac Newton Group[8] (Figure 2).

UT	AirT	Hum	Wspd	Gust	Wdir	Press	LocT	wht.T	Mirr	LocRH	wht.RH
	degC	%	km/s	km/s	deg	mbar	degC	degC	degC	%	%
21:00	11.8	9	1.4	1.8	151	769.4	11.8	11.	10.	9	21
22:00	11.6	7	3.6	3.9	73	769.5	11.6	11.	10.	7	19
23:00	11.2	8	6.2	6.9	120	769.9	11.2	10.	10.	8	20
00:00	11.2	8	11.4	12.9	164	770.1	11.2	10.	10.	8	19
01:00	11.1	8	4.8	11.0	166	769.9	11.1	10.	10.	8	17
02:00	11.3	8	14.2	17.5	144	769.5	11.3	11.	10.	8	17
03:00	11.8	9	10.9	11.8	129	769.1	11.8	11.	10.	9	18
04:00	11.7	9	10.9	11.4	157	768.7	11.7	10.	10.	9	18
05:00	11.9	7	9.2	10.8	112	768.5	11.9	10.	10.	7	19
06:00	12.4	7	10.7	14.0	109	768.5	12.4	9.	10.	7	20

TIME LOST weather 00:00
TIME LOST Technical 00:00
TIME LOST Other 00:00

WEATHER CONDITIONS (eg transparancy, dust, %cloud cover, seeing):
occasional high cirrus, variable seeing

COMMENTS (causes of time lost, setup information eg CCD windows):
Drift of 2" in RA in 2 hours while guiding, switch to other reference star
seemed to solve it (though airmass at that point was very low)
Some bias features visible in ACAM...

Figure 2: *Precise weather and observation conditions at the time the data set was taken, provided by the Isaac Newton Group.*

The complete data set contained two sets of bias fields (120 and 25 files each), two sets of flat fields (17 and 28 files each) and a set of GJ1214 observations (364 files). The first set of biases was taken between 14:56 and 15:02 (UT) and the second set was taken between 5:55 and 6:01 (UT) with 0.0 seconds of exposure time. The first set of flat fields was taken between 20:27 to 20:37 (UT) and 5:38 to 5:51 (UT) with varying exposure times in the range of 2.0 – 32.0 seconds. Finally, the GJ1214 data was taken between 23:59 and 4:25 (UT) with a 30.0 second exposure time for each observation. The data files

themselves are .fit files that contain optical images of a circular field of view in which the target star (GJ1214) as well as other reference stars are located. The primary source of systemic error is from the variation of sensitivity in the detector at each pixel as well as dark current which are discussed in further detail in the next section.

4 Data Reduction and Methods

The first stage of this experiment involves correcting the GJ1214 data using the provided bias and flat field frames. A bias frame is used to measure the noise that the detector reads when there is no actual signal; this is excess noise that must be removed as it is not a consequence of any physical phenomenon that is relevant to the experiment. Flat frames on the other hand measure how the sensitivity of the detector varies pixel-to-pixel, which is important to account for as we want each pixel to be calibrated to the same sensitivity to give accurate measurements. To correct the data, the median (across all of the bias/flat field files) of each pixel is computed for the bias and flat field frames as well as the average value of the flat field corrected image. Each image can then be corrected using the equation[3]:

$$C_i = \frac{R_i - B}{F - B} M \tag{1}$$

$$G = \frac{M}{F - B} \tag{2}$$

Where C_i is the corrected i^{th} image, R_i is the i^{th} raw image, B is the median bias frame, F is the median flat field frame, M is the average pixel value of $(F - B)$ and G is the gain. Note that all of the flat field images were first normalized to be the same flux before applying this correction. Also any flat fields with an exposure time under 10.0 seconds were not used in favour of increased quality in the flat field sensitivity correction. Additionally, due to the field of view for the detector being circular, the edges of the data set are not relevant as they are not part of the observation. As such a vignette was created for each image to mask out the areas that are not in the field of view (see Appendix for the specifics of how this was coded).

With this corrected data, the next step is to selected reference stars so that the flux of the target star (GJ1214) can be compared to other stars as this reduces the variation due to other sources that are not relevant to the transit in the system. The six brightest (and unsaturated) stars in the field of view were selected as the references stars and their position (in terms of pixels) was manually found for the first and last frame; the shift was only by a few pixels in both x and y directions. It was assumed (since the exposure time for each observation frame was the same, 30.0 seconds) that these stars moved at a constant rate along the sky and using the initial and final positions, the rate of change in each reference

star's position was computed and applied to find their position in each frame. Similarly, the position of the target star was tracked through all 364 observation frames.

Aperture photometry is used to measure the flux of the GJ1214 system throughout the range of provided images to find a transit. In this technique an aperture of a defined radius is created around the star by masking out everything that isn't within that radius and integrating within the aperture to find the total flux coming from the star. The optimal radius for an aperture is estimated by plotting the ratio of total flux over noise for varying radii (details in section 5), where the noise is approximated from an annulus outside of the aperture radius that contains no bright sources.

Using this technique to compute the flux for the reference and target stars, the relative flux of the target with respect to the reference stars is plotting over time and the transit of GJ1214b is characterized by a decrease in relative flux as the planet blocks some of the light from reaching the detector.

This light curve is then used to determine properties of the GJ1214 system and in particular GJ1214b (the planet). Firstly, since dip in flux is caused directly by the geometric projection of one object moving in front of another bright object, then given the radius of the parent star, one can compute the radius of the planet from the equation[10]:

$$\delta = \frac{\Delta F}{F} = \left(\frac{R_p}{R_*}\right)^2 \tag{3}$$

Where δ is the fractional change in flux of the target star, R_p is the radius of the planet and R_* is the radius of the parent star. Furthermore, given the mass of the planet, it is simple to compute the density of the planet[2] (which characterizes what type of planet it is, i.e. Earth-like, gas giant, etc.):

$$M_p = \frac{4}{3}\pi R_p^3 \rho_p \quad \Longrightarrow \quad \rho_p = \frac{3}{4}\frac{M_p}{\pi R_p^3} \tag{4}$$

Where M_p and ρ_p are the mass and density of the planet respectively. Additionally, by finding the ingress and egress of the transit, it is possible to determine the inclination angle of the system and the period of the planet's orbit around its parent star[10].

$$P = \frac{M_*}{R_*^3}\frac{G\pi}{32}\frac{(t_T^2 - t_F^2)^{3/2}}{\delta^{3/4}} \tag{5}$$

$$i = \cos^{-1}\left(\frac{bR_*}{a}\right) \tag{6}$$

$$where \quad a = \frac{2PR_*\delta^{\frac{1}{4}}}{\pi(t_T^2 - t_F^2)^{\frac{1}{2}}} \quad and \quad b = \left(\frac{\left(1 - \delta^{\frac{1}{2}}\right)^2 - \left(\frac{t_F}{t_T}\right)^2 \left(1 + \delta^{\frac{1}{2}}\right)^2}{1 - \left(\frac{t_F}{t_T}\right)^2} \right)^{\frac{1}{2}} \tag{7}$$

Where P is the period of orbit, t_F is the full depth eclipse duration, t_T is the transit duration, i is the inclination angle, b is the impact parameter and a is the orbital distance.

Lastly a limb darkening affect is applied to the light curve to more accurately depicts the decrease in flux near the edges of the star compared to the center (due to optical depth and effective temperature changing between the center and edge of a star)[5]. The new light curve is then analyzed and compared to the original one without limb darkening effects in section 6.

The largest source of error throughout the analysis and modeling section arises from the background noise in the image (i.e. the average flux of background pixels where there is no astronomical source in the line of sight) and Poisson noise which is derived from the gain of the detector. There is also the systemic error that was corrected using bias and flat fields before generating the light curve.

5 Data Analysis and Modeling

The detailed python code for generating all figures and data analysis in this section can be found in the Appendix. To start, the median of the bias and flat field frames were computed and used to correct the data as mentioned in the previous section (Figure3). This reduces the systemic noise present in the data and allows for a more accurate measurement of flux.

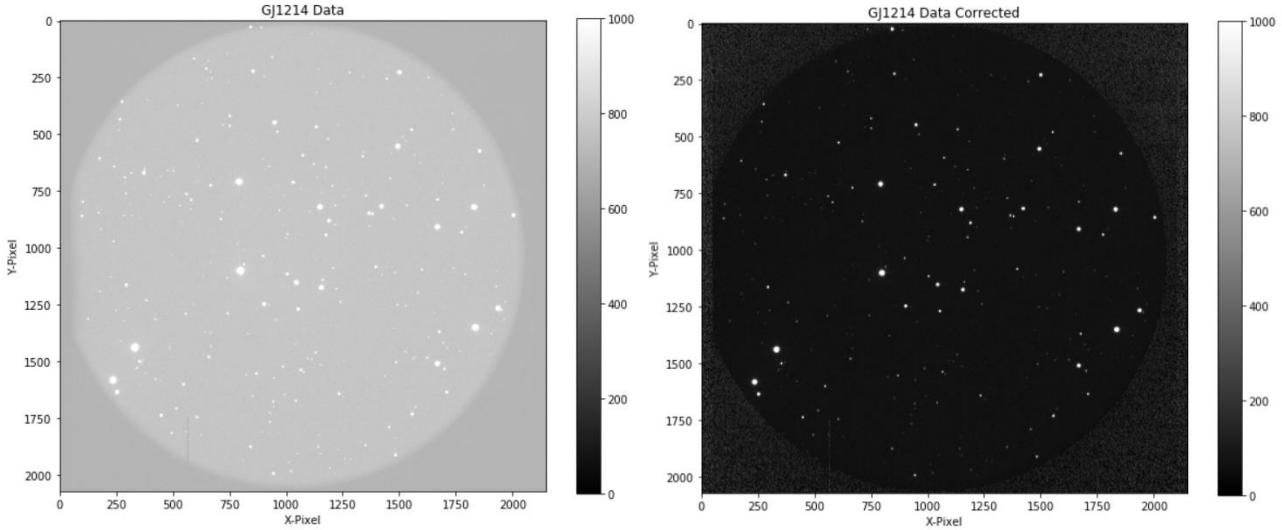

Figure 3: *a) (Left) The WHT ACAM optical image without any corrections applied, b) (Right) The same optical image but with the bias and flat field corrections applied.*

Additionally, a circular mask was applied to the data to account for the fact that the field of view is circular and thus we do not want the external points that do not correspond to points in the sky to contribute to the data. Note that the field of view wasn't exactly circular so the mask was applied with a radius that reached the vertical cut-off on the left side and as a result some data on the outer edges was lost but those points are not significant to this experiment. Then, using an existing catalog, the target star was identified and the six brightest stars were identified to be used as the reference stars. The central position of these seven stars was found manually in the first frame (Figure 4).

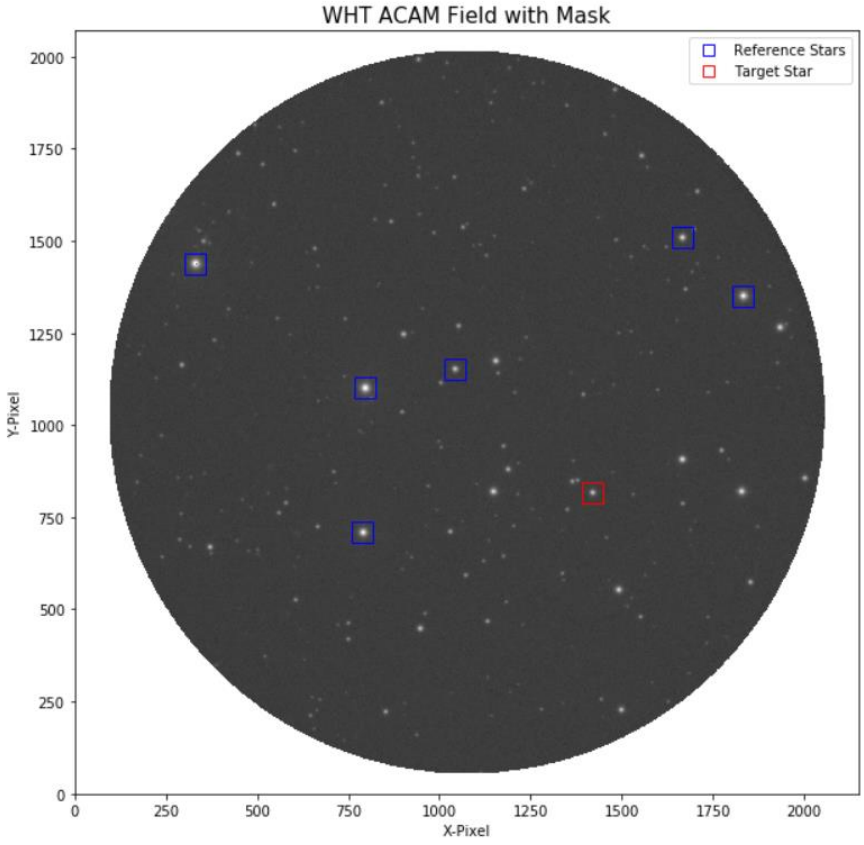

Figure 4: *The WHT ACAM optical image now with a circular mask applied and reference/target stars selected.*

As mentioned in the previous section, the central positions of all of these stars was also found in the final optical frame such that the rate of change in each star's position could be computed to correctly track the star through all 364 frames. A short table summarizing the initial pixel positions of these stars can be found in the Appendix (Table 1).

Aperture photometry can then be used to analyze the corrected data but first and optimal aperture radius must be computed for the target star. This is done through computing the ratio of the total integrated flux within the aperture over total noise as a function of aperture radius (Figure 5). The

aperture itself and the background annulus are created by locating the target star and masking out regions to define an aperture and annulus (for background noise) (Figure 6). It was found that, for the target star, the optimal aperture radius is approximately 6 pixels. Similarly, this process was repeated on the reference stars and their optimal aperture radius ranged between 6 and 8 pixels (Table 1).

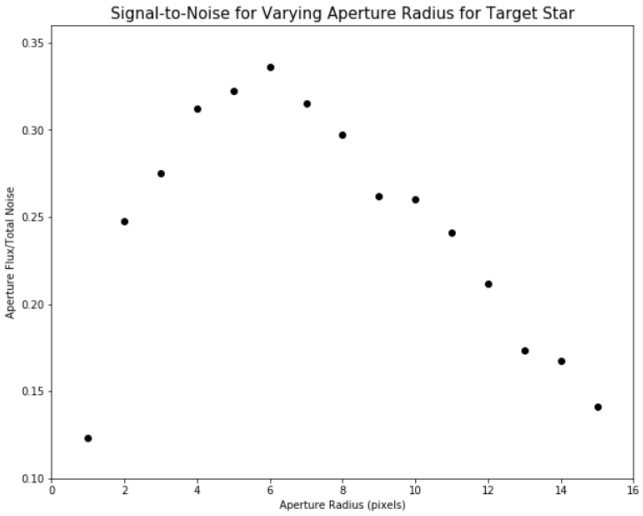

Figure 5: *Aperture Flux/Total Noise plotted against Aperture Radius to approximate the optimal aperture radius for the aperture photometry analysis.*

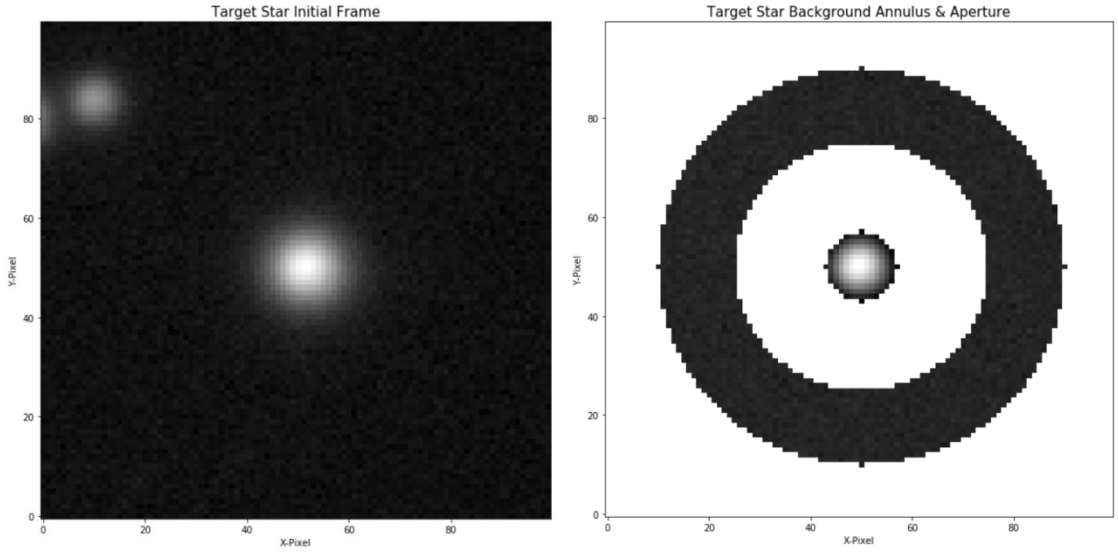

Figure 6: *a) (Left) An enhanced image of the target star, b) (Right) Inner circle is an aperture (radius = 6 pixels) around the target star and outer ring is an annulus used to compute background noise (inner radius = 25 pixels, outer radius = 40 pixels).*

Furthermore, using the optimal aperture radius, the flux of the target and reference stars is measured as the integrated flux over their respective apertures. A light curve is then generated by taking the ratio of the target star's flux over the average reference star flux and plotting it against time (Figure 7).

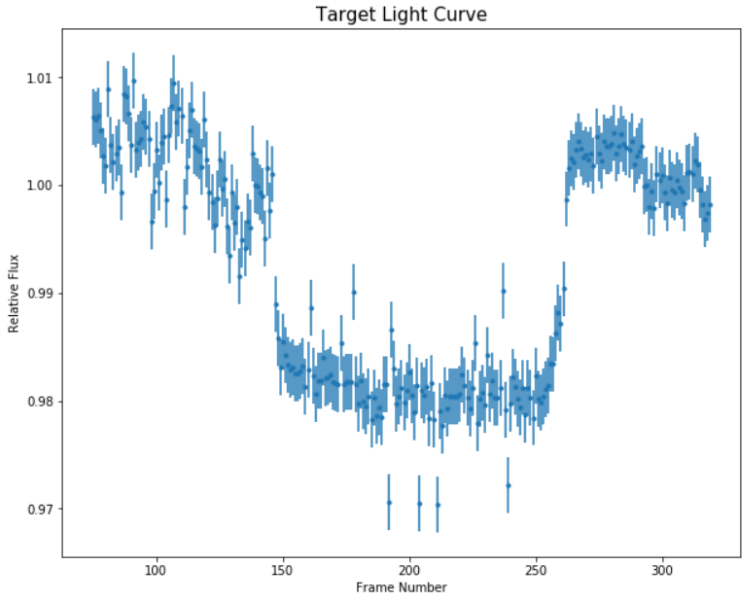

Figure 7: *GJ1214 system light curve; relative flux of the target star with respect to reference stars plotted against the frame number, which directly corresponds to time of the observation. Only the region around the transit is plotted as this is the primary interest in the light curve.*

Computing the parameters from the system using the light curve gives that $\delta \cong 0.022 \pm 0.005$ and then using equation (3) with $R_* \cong 0.216 \pm 0.012\ R_{sun}$ [7] gives that $R_p \cong 0.319 \pm 5.74\ R_J$. Thus, given the mass of the planet ($M_p \cong 0.020 \pm 0.003\ M_J$)[7], and the measured radius, R_p, the density of the planet is computed using equation (4) to give $\rho_P \cong 832 \pm 10731\ kg/m^3 = 0.832 \pm 10.731\ g/cm^3$. Furthermore, approximating the ingress and egress with the given timestamps corresponding to the frame numbers it is found that $t_T = 5280 \pm 150\ s$ and $t_F = 4380 \pm 150\ s$. Using these values, the period and inclination angle are measured using equations (5-7), leading to: $P \cong 0.70 \pm 9.03\ days$, $a = 1.12\ x\ 10^8 \pm 3.59\ x\ 10^8\ m$, $b \cong 0.397 \pm 0.973$ and therefore $i \cong 85.5 \pm 27.5^o$.

6 Discussion

Firstly, discussing the systemic error correction using bias and flat fields as well as a circular vignette, it is clear from Figures 3 and 4 that this calibration reduces the overall noise in the data set and allows for a much clearer view of the stars in the field which also makes it easier to find their locations. This correction makes the background counts very close to zero; not exactly but they are very small in comparison to the stars that are present. The apparent size of stars in this image varies but is roughly a few pixels in radius (on the scale of 1 to 10 pixels), although the real size of the stars is smaller since not the entire illuminated circle that is seen would be within the star's actual radius.

The reference stars are selected as the six brightest stars in the field that do not correspond to a known variable star (Figure 4). As mentioned earlier, the stars' central location was found manually for the first and last frame; it was assumed that the motion was constant and a simple rate of change was applied to each star to track it throughout the data set.

From Figure 5 it is clear that for the target star the optimal aperture radius is 6 pixels. This is because below 6 pixels not all of the flux from the star is captured within the aperture. Especially at very small radii (i.e. 1 or 2) it is clear that such a small aperture is not representative of the flux of the observed star. For radii greater than 6 pixels, the ratio of total aperture flux over total noise begins to decrease because more and more background pixels are being added into the aperture. After a certain point (6 pixels) the entire star's flux is within the aperture and increasing the aperture size will only add background noise. A visualization of this is seen in Figure 6 where the aperture radius is 6 pixels and the annulus around it is used to compute the background noise. The same technique was applied to optimize the aperture radii of the reference stars which vary slightly just slightly from the target star as their apparent size isn't exactly the same.

The light curve seen in Figure 7 shows a clear transit pattern in the relative flux drops down for some time and then returns. The resulting values can be compared to the expected results and analyzed. It was observed that $R_p \cong 0.319 \pm 5.74\ R_J$ while the expected value is $0.238 \pm 1.071\ R_J$[7]; the observed result is within the error margins of the expected and is overall fairly close. Similarly, $\rho_P = 0.832 \pm 10.731\ g/cm^3$ while the expected result is approximately $1.99 \pm 0.87\ g/cm^3$[7], which is again fairly similar and we can be confident that the observed result is reasonable. The observed values for period and inclination angle were: $P \cong 0.70 \pm 9.03\ days$ and $i \cong 85.5 \pm 27.5^o$ whereas the expected values are $1.58 \pm 1.8\ x\ 10^{-7}\ days$ and 88.17 ± 0.54^o respectively[7]. The observed inclination angle is very similar to the expected but the orbital period differs by a factor of approximately two.

Through these observed values it can be determined that GJ1214b is a large planet roughly a third of Jupiter's radius (roughly 3.5 times larger than Earth's radius, thus it can be dubbed a "Super-Earth" in this radius range) with density similar to that of a gas giant. It has a very short orbital period of roughly a day and is extremely close to the parent star ($a = 1.12\ x\ 10^8 \pm 3.59\ x\ 10^8\ m$). Additionally the parent star is a dim red dwarf star with estimated surface temperature of $3000\ K$. Thus, due to the very close proximity of the exoplanet to its star it can be theorized that the surface temperature of the planet would also be considerably high (a few hundred K).

A limb darkening correction was attempted for the light curve of the GJ1214 system, however the resulting light curve became very noisy and had little to no effect on the shape of the light curve. As such it was deemed that this analysis does not accurately depict the effect limb darkening has on the observation and would lead to no additional discussion and was thus excluded from this section.

7 References

[1] Been et al. 2008, Society of Photo-Optical Instrumentation Engineers (SPIE) Conference Series, Vol. 7014

[2] Borucki et al., 2010, The Astrophysical Journal Letters, 713, L126, http://arxiv.org/abs/1001.0604

[3] Carroll B. W., Ostlie D. A. 1996, Weber State University, Ogden, Utah. "An Introduction to Modern Astrophysics",

[4] Centre de Données astronomiques de Strasbourg, Strasbourg Observatory, France 2019, "Aladin Sky Atlas", https://aladin.u-strasbg.fr/

[5] Claret 2004, Astronomy & Astrophysics, 428, 1001, https://www.aanda.org/articles/aa/abs/2004/48/aa1673/aa1673.html

[6] Czech Astronomical Society 2019, "Exoplanet Transit Database", http://var2.astro.cz/ETD/

[7] Exoplanet TEAM 2019, "The Extrasolar Planets Encyclopedia", http://exoplanet.eu/

[8] Isaac Newton Group of Telescopes 2019, "William Herschel Telescope", http://www.ing.iac.es/Astronomy/telescopes/wht/

[9] Mandel & Agol 2002, The Astrophysical Journal Letters, 580, L171, http://arxiv.org/abs/astro-ph/0210099

[10] Sackett 1999, "Planets outside the Solar System: theory and observations", NATO-ASI Series, http://arxiv.org/abs/astro-ph/9811269

[11] Seager & Mallen-Nornelas 2003, The Astrophysical Journal, 585, 1038, http://arxiv.org/abs/astro-ph/0206228

8 Appendix

8.1 Initial Pixel Positions and Optimal Aperture Radius of Reference and Target Stars

Table 1: *Initial Position Parameters and Aperture Radius for Selected Stars.*

Object	Initial X-Pixel	Initial Y-Pixel	Aperture Radius
Reference Star 1	330	1439	8
Reference Star 2	795	1102	8
Reference Star 3	788	710	7
Reference Star 4	1831	1351	7

Reference Star 5	1664	1510	6
Reference Star 6	1041	1153	6
Target Star (GJ1214)	1419	817	6

8.2 Python Code for Systemic Corrections of Bias/Flat Fields and Masking (Figures 3-4)

Note that this section of code walks through how to apply the corrections to one frame; these corrections were looped to be applied to all frames but that is not included in this code as it would be repetitive.

```
#AST326 Lab 5 – Detecting Exoplanet Transits
#Ayush Pandhi (1003227457)
#March 20, 2019

#Importing required modules
import numpy as np
from matplotlib import pyplot as plt
from astropy.io import fits

#Loading the Set of Bias Data
Bias_index = np.arange(0, 21)
Bias = []
Biasdata = []
for i in Bias_index:
    Bias = fits.open('/Users/ayush/Desktop/School/University/Third Year/AST326/Lab 5/Lab5_ACAM_DATA/r' + str(Bias_index[i]+1599995) + '.fit')
    Biasdata.append(Bias[1].data)
Biasdata = np.array(Biasdata)

#Getting the Median of the Bias Data
Biasdata_median = np.median(Biasdata, axis=0)

#Plotting 2D Median of Bias Data
plt.figure(figsize=(10,8))
plt.imshow(Biasdata_median, cmap='gist_gray')
plt.title('Bias Spectra')
plt.xlabel('X-Pixel')
plt.ylabel('Y-Pixel')
plt.colorbar()
```

```
plt.show()

#Loading the Set of Flat Field Data
Flat_index = np.arange(0, 28)
Flat = []
Flatdata = []
for i in Flat_index:
    Flat = fits.open('/Users/ayush/Desktop/School/University/Third Year/AST326/Lab 5/Lab5_ACAM_DATA/r' + str(Flat_index[i]+1599966) + '.fit')
    Flatdata.append(Flat[1].data)
Flatdata = np.array(Flatdata)

#Normalizing and Getting the Median of the Flat Fields
Flatdata_norm = Flatdata/np.median(Flatdata, axis=0)
Flatdata_median = np.median(Flatdata_norm, axis=0)

#Plotting 2D Median of Flat Field Data
plt.figure(figsize=(10,8))
plt.imshow(Flatdata_median, cmap='gist_gray')
plt.title('Flat Field Spectra')
plt.xlabel('X-Pixel')
plt.ylabel('Y-Pixel')
plt.colorbar()

#Testing on the First GJ1214 Data Frame
GJ1214 = fits.open('/Users/ayush/Desktop/School/University/Third Year/AST326/Lab 5/Lab5_ACAM_DATA/r1599579.fit')
GJ1214data = GJ1214[1].data

#Plotting 2D GJ1214 data without corrections
plt.figure(figsize=(10,8))
plt.imshow(GJ1214data, cmap='gist_gray', vmax=1000, vmin=0)
plt.title('GJ1214 Data')
plt.xlabel('X-Pixel')
plt.ylabel('Y-Pixel')
plt.colorbar()
plt.show()
```

```
#Subtracting off bias and dividing by flat
GJ1214data_fix = (GJ1214data - biasdata_mean)/flatdata_mean

#Plotting 2D GJ1214 data
plt.figure(figsize=(10,10))
plt.imshow(GJ1214data_fix, cmap='gist_gray', vmax=1000, vmin=0)
plt.title('WHT ACAM Field After Corrections', fontsize=15)
plt.xlabel('X-Pixel', fontsize=10)
plt.ylabel('Y-Pixel', fontsize=10)
plt.show()

#Creating a Circular Mask
c = [int(2071/2), int(2148/2)]    #center of image
Y, X = np.ogrid[:2071, :2148]
d = np.sqrt((X - c[0])**2 + (Y - c[1])**2)   #array of distances from the center
circmask = d <= 980  #mask such that the distances must be less than the vertical cutoff on the left

#Applying Mask to First Data Frame and Plotting with Manually Computed Star Locations
GJ1214data_mask = GJ1214data_fix*circmask
plt.figure(figsize=(10,10))
plt.imshow(np.log10(GJ1214data_mask), aspect='auto', origin='lower', cmap='gist_gray')
plt.plot(330, 1439, 'bs', markersize=15, markerfacecolor='none', label='Reference Stars')
plt.plot(795, 1102, 'bs', markersize=15, markerfacecolor='none')
plt.plot(788, 710, 'bs', markersize=15, markerfacecolor='none')
plt.plot(1831, 1351, 'bs', markersize=15, markerfacecolor='none')
plt.plot(1664, 1510, 'bs', markersize=15, markerfacecolor='none')
plt.plot(1041, 1153, 'bs', markersize=15, markerfacecolor='none')
plt.plot(1419, 817, 'rs', markersize=15, markerfacecolor='none', label='Target Star')
plt.title('WHT ACAM Field with Mask', fontsize=15)
plt.xlabel('X-Pixel', fontsize=10)
plt.ylabel('Y-Pixel', fontsize=10)
plt.legend(markerscale=0.5)
plt.show()
```

8.3 Python Code for Aperture Photometry (Figures 5-6)

Again the code below is only for the aperture analysis on one frame. The same process was applied to each frame but not included here as it would be repetitive.

```
#Using Initial and Final Target Center for Tracking
GJ1214_xvel = (GJ1214_xf – GJ1214_xi)/(GJ1214_time[364] – GJ1214_time[0])
GJ1214_yvel = (GJ1214_yf – GJ1214_yi)/(GJ1214_time[364] – GJ1214_time[0])

#Getting the x and y Pixel Positions for each Frame
GJ1214_x = np.zeros(364)
G1214_y = np.zeros(364)
for i in range(0, 364):
  if i = 0:
    GJ1214_x[i] = GJ1214_xi
    GJ1214_y[i] = GJ1214_yi
  else:
    GJ1214_x[i] = GJ1214_xi + int(GJ1214_xvel*(GJ1214_time[i] – GJ1214_time[i-1]))
    GJ1214_y[i] = GJ1214_yi + int(GJ1214_yvel*(GJ1214_time[i] – GJ1214_time[i-1]))

#Use Masking Procedure to Create Aperture
d2 = np.sqrt((X – GJ1214_x[0])**2 + (Y – GJ1214_y[0])**2)
Annulus_outer_GJ1214 = d2 <= 40
Annulus_inner_GJ1214 = d2 >= 25
Annulus_GJ1214 = GJ1214data_fix*Annulus_outer_GJ1214*Annulus_inner_GJ1214
Aperture_outer = d2 <= 6
Aperture_GJ1214 = GJ1214data_fix*Aperture_outer

#Computing Aperture Flux and Correcting for noise
GJ1214_apflux = np.sum(Aperture_GJ1214)
bg_noise = np.sum(Annulus_GJ1214)
bg_noise_perpixel = bg_noise/(np.pi*(40**2) – np.pi*(25**2))
GJ1214_apflux_fix = GH1214_apflux – bg_noise_perpixel – p_noise_perpixel   #p_noise is poisson noise from before when the systemic corrections were made

#Finding Optimal Aperture Radius By Repeating Above Steps for Various Radii
r_test = np.arange(1, 16)
Aperture_outertest = []
Aperture_test = []
Apflux_test = []
```

```
APflux_fix_test = []
for i in r_test:
    Aperture_outertest.append(d2 <= r_test[i])
Aperture_outertest = np.array(Aperture_test)
for i in r_test:
    Aperture_test.append(GJ1214data_fix*Aperture_outertest[i])
Aperture_test = np.array(Aperture_test)
for i in r_test:
   Apflux_test.append(numpy.sum(Aperture_test[i]))
Apflux_test = np.array(Apflux_test)
for i in r_test:
   Apflux_fix_test.append(Apflux_test[i] – bg_noise_perpixel – p_noise_perpixel)
Apflux_fix_test = np.array(Apflux_fix_test)

#Plotting Singnal to Noise for Varying Radii
plt.figure(figsize=(10,8))
plt.plot(r_test, Apflux_fix_test/(bg_noise + p_noise), 'k.', markersize=12)
plt.title('Signal-to-Noise for Varying Aperture Radius for Target Star', fontsize=15)
plt.xlabel('Aperture Radius (pixels)', fontsize=10)
plt.ylabel('Aperture Flux/Total Noise', fontsize=10)
plt.xlim(0,16)
plt.ylim(0.10, 0.36)
plt.show()

#Plotting Zoomed In Target
plt.figure(figsize=(10,10))
plt.imshow(np.log10(GJ1214data_mask[817-50:817+50,          1419-50:1419+50]),          aspect='auto',
origin='lower', cmap='gist_gray')
plt.title('Target Star Initial Frame', fontsize=15)
plt.xlabel('X-Pixel', fontsize=10)
plt.ylabel('Y-Pixel', fontsize=10)
plt.show()

#Plotting Aperture/Annulus
plt.figure(figsize=(10,10))
plt.imshow(np.log10(Annulus_GJ1214), aspect='auto', origin='lower', cmap='gist_gray')
plt.imshow(np.log10(Aperture_GJ1214), aspect='auto', origin='lower', cmap='gist_gray')
plt.title('Target Star Background Annulus & Aperture', fontsize=15)
```

```
plt.xlabel('X-Pixel', fontsize=10)
plt.ylabel('Y-Pixel', fontsize=10)
plt.show()
```

8.4 Python Code for Plotting the Light Curve (Figure 7)

Once the above aperture analysis is completed for all reference stars and target star for all 364 frames, the relative flux of the target to the mean flux of all reference stars (which is roughly constant over time) is plotted to see a transit.

```
#Get Relative Flux Ratio of Target to the Mean Background Fluxes
GJ1214_relflux = np.zeros(364)
for i in range(0, 364):
    GJ1214_relflux[i] = GJ1214_apflux_fix_all[i]/Ref_apflux_all_mean[i]

#Plotting the Light Curve in the Area of the Transit
plt.figure(figsize=(10,8))
plt.errorbar(np.arange(75, 320), GJ1214_relflux[75:320], xerr=None, yerr=GJ1214_relflux_error[75:320],
ls='', marker='o', markersize=3)
plt.title('Target Light Curve', fontsize=15)
plt.xlabel('Frame Number', fontsize=10)
plt.ylabel('Relative Flux', fontsize=10)
```